Implementation of Taguchi Design for Erosion of Fiber-Reinforced Polyester Composite Systems with SiC Filler

First published on March 19, 2008

Journal of Reinforced Plastics and Composites 2008

http://dx.doi.org/10.1177/0731684407087688

Implementation of Taguchi Design for Erosion of Fiber-Reinforced Polyester Composite Systems with SiC Filler

AMAR PATNAIK*
Department of Mechanical Engineering, National Institute of Technology Hamirpur-177005, India

ALOK SATAPATHY AND S. S. MAHAPATRA
Department of Mechanical Engineering, National Institute of Technology Rourkela-769008, India

R. R. DASH
Department of Mechanical Engineering, G.I.E.T, Gunupur-765022, India

ABSTRACT: With the increased use of fiber/filler-reinforced polymer composites in erosive work environments, it has become extremely important to investigate their erosion characteristics intensively. This article describes the development of a multi-component composite system consisting of thermoplastic polyester resin reinforced with E-glass fiber and SiC particles, and studies its erosion behavior under different operating conditions. A room temperature erosion test facility and Taguchi's orthogonal arrays are used for experimentation. It identifies significant control factors influencing the erosion wear and also outlines significant interaction effects. Finally, optimal factor settings for minimum wear rate have been determined using a genetic algorithm.

KEY WORDS: E-glass fiber, SiC, Taguchi method, GA.

INTRODUCTION

FIBER-REINFORCED POLYMER COMPOSITES have many applications in automobile, marine, and aerospace industries. Due to operational requirements in dusty environments, the erosion characteristics of these composites are of vital importance. Since erosive wear of engineering components caused by abrasive particles is a major industrial problem, a full understanding of the effects of all system variables on the wear rate is necessary in order to undertake appropriate steps in the design of machine or structural components, and to choose the materials to reduce/control this wear mode. In recent years much research has been devoted to exploring the potential advantages of thermoplastic polymers for composite materials. Some of the commonly used thermoplastics are polyetheretherketone (PEEK), polyetherketone (PEK), polyetherketoneketone (PEKK), polyester, polypropylene (PP), etc. Several investigations on friction and wear properties of PEEK and its composites filled with fibers, organic, and inorganic fillers have been carried out [1,2]. Cirino et al. [1,3] reported the sliding as well as

*Author to whom correspondence should be addressed. E-mail: amar_comp4@rediffmail.com

the abrasive wear behavior of continuous carbon and aramid fiber-reinforced PEEK. Lhymn et al. [4] have studied the abrasive wear of short carbon fiber-reinforced PEEK. Voss and Friedrich [5] investigated the sliding and abrasive wear behavior of short fiber-reinforced PEEK composites at room temperature. Briscoe et al. [6] described the friction and wear of PEEK-PTFE blends over a wide composition range under several testing conditions. Bahadur and Gong [7] investigated the action of various copper compounds as fillers on the tribological behavior of PEEK. Wang et al. [2,8,9] investigated friction and wear properties of nanometric ZrO_2 and SiC-filled PEEK composites with different filler proportions. Most of the above studies are confined to dry sliding of PEEK and its composites. The erosive wear behavior of polyester composites reinforced with any fiber or particulate has not yet been reported in the literature.

Hard particulate fillers consisting of ceramic or metal particles and fiber fillers made of glass are being used these days to dramatically improve the wear resistance, even up to three orders of magnitude [10]. The improved performance of polymers and their composites in tribological applications by the addition of filler materials has shown great promise and so has lately been a subject of considerable interest. Various kinds of polymers and polymer matrix composites reinforced with metal particles have a wide range of industrial applications, such as heaters, electrodes [11], composites with thermal durability at high temperature [12], etc. These engineering composites are desired due to their low density, high corrosion resistance, ease of fabrication, and low cost [13–15]. Similarly, ceramic-filled polymer composites have been the subject of extensive research in the last two decades. The inclusion of inorganic fillers into polymers for commercial applications is primarily aimed at cost reduction and stiffness improvement [16,17]. Along with fiber-reinforced composites, the composites made with particulate fillers have been found to perform well in tribological conditions.

Silicon carbide (SiC) is one such ceramic material that has the potential to be used as filler in various polymer matrices. It is an excellent abrasive and has been produced and made into grinding wheels and other abrasive products for over 100 years. It is the only chemical compound of carbon and silicon. It was originally produced by a high temperature electro-chemical reaction of sand and carbon. Today the material has been developed into a high quality technical grade ceramic with very good mechanical properties. It is used in abrasives, refractories, ceramics, and numerous high performance applications. The material can also be made an electrical conductor and has applications in resistance heating, flame igniters, and electronic components. Structural and wear applications are constantly developing. Silicon carbide is composed of tetrahedra of carbon and silicon atoms with strong bonds in the crystal lattice. This produces a very hard and strong material. It is not attacked by any acids, alkalis, or molten salts up to 800°C. The high thermal conductivity coupled with low thermal expansion and high strength gives this material exceptional thermal shock resistant qualities. Silicon carbide has low density of about 3.1 g/cm^3, low thermal expansion, high elastic modulus, high strength, high thermal conductivity, high hardness, excellent thermal shock resistance, and superior chemical inertness.

The experimental strategy has been adapted from the methodology outlined for successful parametric appraisal in other applications like wire electrical discharge machining (WEDM) process, drilling of metal matrix composites, and erosion behavior of metal matrix composites such as aluminum-reinforced with red mud by Mahapatra and Patnaik [18–20]. Also Patnaik et al. [21] report on erosion behavior of glass fiber-polyester composites filled with a filler material called flyash. As flyash is abundantly

available as industrial waste and cheap, the study finds the possibility of using flyash as filler material and characterizes wear behavior. This article reveals that addition of flyash improves the erosion performance of polyester composite to a certain extent. Again Patnaik et al. [22] focus on characterization of wear behavior of polymer matrix composites without addition of any filler material. The previous studies demonstrate that addition of filler material improves the erosion properties of polymer matrix composite but degrades some mechanical properties, notably tensile strength. Better tensile strength properties can be obtained without adding any filler material. Further, Patnaik et al. [23] suggest that alumina is a good candidate to be used as filler material in glass fiber-reinforced polyester composites. The erosion wear of composite reduces by many folds with addition of alumina, in comparison to wear characteristics of unfilled composites. In order to reduce the number of experiments and proceed with the experimental procedure in a systematic manner, the Taguchi method has been adopted in all three investigations. The Taguchi method helps to ease the process of analyzing the experimental results and get insight into the physical phenomenon of experimentation. Since the Taguchi method is used as an analyzing tool in all cases, they seem to be similar. It should be noted that the objectives of all the articles are quite different and the focus of each study differs from the others.

In view of the above, the objective of the present investigation is to study the effect of glass fiber reinforcement and inclusion of SiC filler on the erosive wear behavior of polyester under multiple impact conditions. An attempt is made to optimize the process parameters for minimum erosion. An evolutionary approach known as the genetic algorithm has also been applied in the present study for the determination of optimal factor settings to minimize the erosion rate.

EXPERIMENTAL DETAILS

Composite Fabrication

Cross-plied E-glass fibers (360 roving taken from Saint Govion) are reinforced in SiC-filled unsaturated isophthalic polyester resin to prepare the composites. The composite slabs are made by conventional hand lay-up technique. Two percent cobalt nephthalate (as accelerator) is mixed thoroughly in isophthalic polyester resin and then 2% methyl-ethyl-ketone-peroxide (MEKP) as hardener is mixed in the resin prior to reinforcement. The filler material SiC is provided by NICE Ltd, India. E-glass fiber and polyester resin have modulus of 72.5 and 3.25 GPa, respectively, and possess densities of 2590 and 1350 kg/m^3, respectively. Composites of three different compositions (0, 10, and 20 wt% SiC filling) are made and the fiber-loading (weight fraction of glass fiber in the composite) is kept at 50% for all the samples. The castings are put under load for about 24 h for proper curing at room temperature. Specimens of suitable dimension are cut using a diamond cutter for physical characterization and erosion testing.

Test Apparatus

Figure 1 shows the schematic diagram of an erosion test rig conforming to ASTM G 76. The setup is capable of creating reproducible erosive situations for assessing erosion wear resistance of the prepared composite samples. It consists of an air compressor, an air particle mixing chamber, and an accelerating chamber. Dry compressed air is mixed with

the particles that are fed at constant rate from a sand flow control knob, through the nozzle tube, and then accelerated by passing the mixture through a convergent brass nozzle of 3 mm internal diameter. These particles impact the specimen, which can be held at different angles with respect to the direction of erodent flow using a swivel and an adjustable sample clip. The velocity of the eroding particles is determined using a standard double-disc method [24]. In the present study, dry silica sand (spherical) of different particle sizes (30, 500, and 80 μm) are used as erodent. The samples are cleaned in acetone, dried, and weighed to an accuracy of ±0.1 mg before and after the erosion trials, using a precision electronic balance. The weight loss is recorded for subsequent calculation of erosion rate. The process is repeated until the erosion rate attains a constant value, called a steady state erosion rate.

Test of Micro-Hardness, Density, Tensile, and Flexural Properties

Micro-hardness measurement is done using a Leitz micro-hardness tester. A diamond indenter, in the form of a right pyramid with a square base and an angle 136° between opposite faces, is forced into the material under a load F. The two diagonals X and Y of the indentation left on the surface of the material after removal of the load are measured and their arithmetic mean L is calculated. In the present study, the load considered $F = 24.54$ N and Vickers hardness number are calculated using the equation:

$$H_V = 0.1889 \frac{F}{L^2} \tag{1}$$

and

$$L = \frac{X + Y}{2}$$

where F is the applied load (N), L is the diagonal of square impression (mm), X is the horizontal length (mm), and Y is the vertical length (mm).

The tensile test is generally performed on flat specimens. The commonly used specimen for the tensile test is the dog-bone specimen and straight-side specimen with end tabs. A uniaxial load is applied at both the ends. The ASTM standard test method for tensile properties of fiber resin composites has the designation D 3039-76. The length of

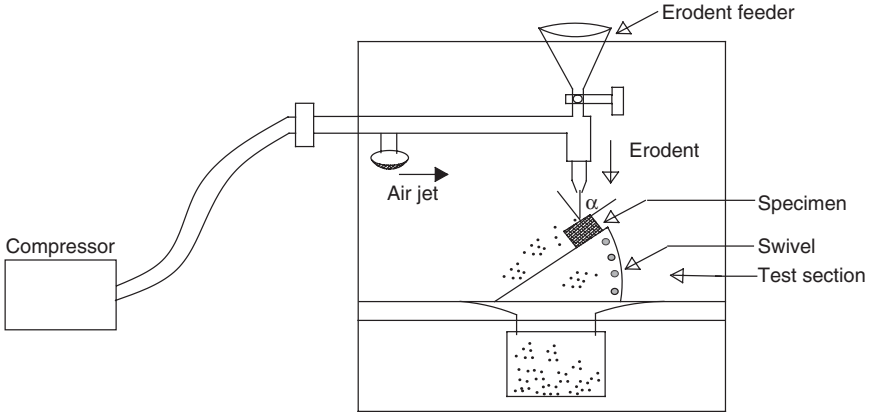

Figure 1. *A schematic diagram of the erosion test rig.*

the test section should be 200 mm. The tensile test is performed in the universal testing machine (UTM) Instron 1195 and results are analyzed to calculate the tensile strength of composite samples. To evaluate the flexural strength, the point bend test is conducted on all the composite samples in the same UTM. A span length of 40 mm and a crosshead speed of 10 mm/min are maintained.

The surfaces of the specimens were examined directly by scanning electron microscope JEOL JSM-6480LV in the LV mode.

Experimental Design

Design of experiment is a powerful analysis tool for modeling and analyzing the influence of control factors on performance output. The most important stage in the design of the experiment lies in the selection of the control factors. Therefore, a large number of factors are included so that non-significant variables can be identified at the earliest opportunity. Exhaustive literature reviews on erosion behavior of polymer composites reveal that parameters, viz., impact velocity, impingement angle, fiber-loading, filler content, erodent size, and stand-off distance, etc, largely influence the erosion rate of polymer composites [25,26]. The impact of five such parameters are studied using L_{27} (3^{13}) orthogonal design. The operating conditions under which erosion tests are carried out are given in Table 1. The standard linear graph, as shown in Figure 2, is used to assign the factors and interactions to various columns of the orthogonal array [27]. In a conventional full-factorial experimental design, it would require $3^5 = 243$ runs to study five parameters each at three levels, whereas Taguchi's factorial experiment approach reduces it to only 27 runs, offering a great advantage in terms of experimental time and cost. The experimental observations are further transformed into signal-to-noise (S/N) ratios. There are several S/N ratios available depending on the type of performance characteristics. The S/N ratio

Table 1. Levels of the variables used in the experiment.

	Level			
Control factor	**I**	**II**	**III**	**Units**
A: Velocity of impact	32	45	58	m/s
B: SiC percentage	0	10	20	%
C: Stand-off distance	120	180	240	mm
D: Impingement angle	45	60	90	degree
E: Erodent size	300	500	800	μm

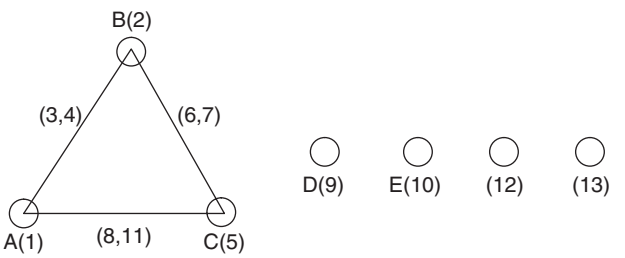

Figure 2. *Linear graphs for L_{27} array.*

for minimum erosion rate can be expressed as 'smaller is better' characteristic, which is calculated as logarithmic transformation of loss function, as shown below:

$$\text{Smaller is better characteristic: } \frac{S}{N} = -10\ \log\frac{1}{n}\left(\sum y^2\right) \tag{2}$$

where n is the number of observations, and y the observed data. The plan of the experiments is as follows: the first column is assigned to impact velocity (A), the second column to SiC percentage (B), the fifth column to stand-off distance (C), the ninth column to impingement angle (D), and the tenth column to erodent size (E); the third and fourth columns are assigned to $(A \times B)_1$ and $(A \times B)_2$, respectively, to estimate interaction between impact velocity (A) and SiC percentage (B), the eight and eleventh columns are assigned to $(A \times C)_1$ and $(A \times C)_2$, respectively, to estimate interaction between the impact velocity (A) and stand-off distance (C), and the remaining columns are used to estimate experimental errors.

RESULTS AND DISCUSSION

Mechanical Properties of Composites

The test results for tensile and flexural strength are shown in Figure 3. It is noticed that as the content of SiC particles increases, both the tensile as well as bending strengths of the composite decline gradually. There is a drop of about 20% in the tensile strength with 10 wt% SiC filling as compared to the unfilled glass-polyester composite. Further, with 20 wt% SiC filling, a reduction of about 30% in composite tensile strength is recorded. The drop in flexural strength with filler content is also gradual but is not as high as that in the case of tensile strength. There can be two reasons for this decline in the strength properties of these particulate-filled composites compared to the unfilled ones. One is that the chemical reaction at the interface between SiC particles and the matrix may be too weak to transfer the tensile/bending stress; the other is that the corner points of the irregular-shaped SiC particles result in stress concentration in the polyester matrix. These two are the factors responsible for reducing the tensile and bending strengths of the composites so significantly. The finding that the strength decreases with increase in filler content further strengthens this phenomenon. However, gradual improvement in tensile modulus of the

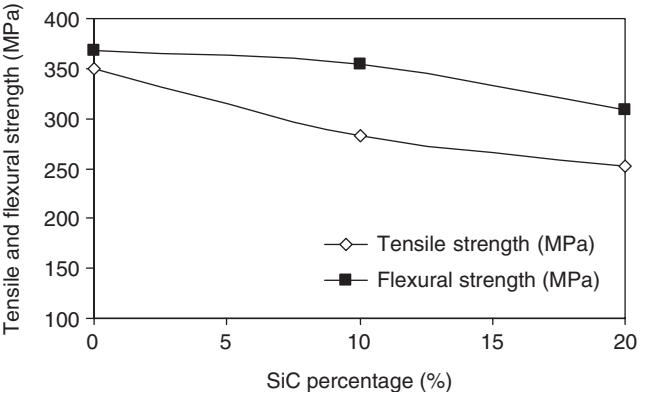

Figure 3. *Effect of SiC filling on tensile and flexural strength of the hybrid composite.*

composites with SiC content is observed (Figure 4), which is attributed to the lower strain rates recorded during the test in the case of the filled composites.

As expected, the hardness values of SiC-GF-polyester composites are found to be higher than the unfilled GF-polyester composite. Again the hardness is seen to have improved with increasing content of SiC (Figure 5). The reduction in tensile strength and the improvement in hardness with the incorporation of filler can be explained as follows: under the action of a tensile force the filler matrix interface is vulnerable to debonding depending on interfacial bond strength and this may lead to a break in the composite. But in the case of the hardness test, a compression or pressing stress is in action. So the thermoplastic matrix phase and the solid filler phase would be pressed together and touch each other more tightly. Thus the interface can transfer pressure more effectively, even though the interfacial bond may be poor. This results in enhancement of hardness. Similar property modification has been observed in the case of the polyurethane matrix composite reinforced with Al_2O_3 particles [28]. The density of the composite is also seen to be varying with increase in filler percentage. This variation is presented in Figure 6. It shows that, initially, density of the composite decreases with addition of SiC particle but beyond 10 wt% the density remains almost constant.

Surface Morphology

From SEM observations of the eroded surfaces, it appears that composites under consideration exhibit several stages of erosion and material removal process.

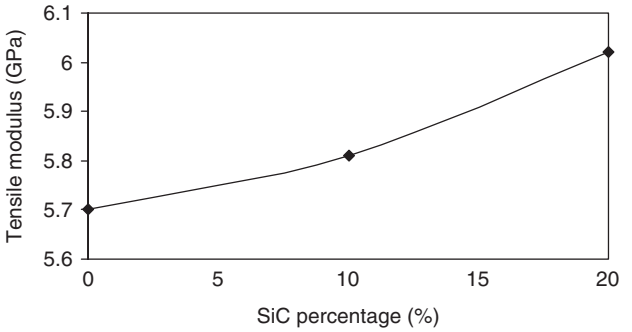

Figure 4. *Effect of SiC filling on tensile modulus of the hybrid composite.*

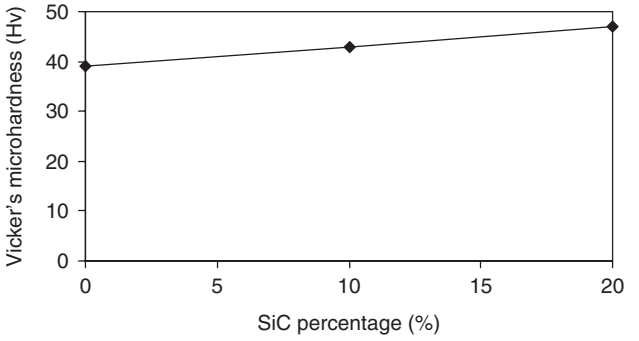

Figure 5. *Variation of Vicker's micro-hardness with SiC percentage.*

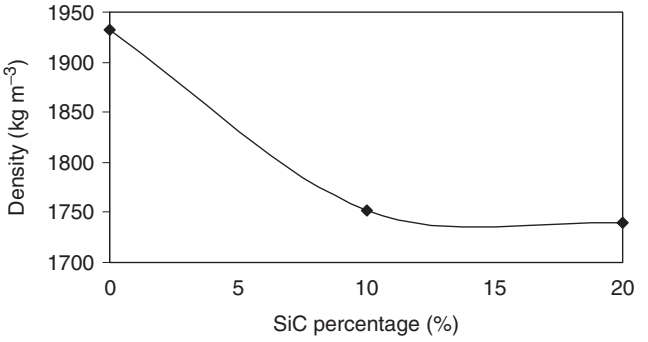

Figure 6. *Effect of SiC filling on density of the hybrid composite.*

Figure 7(a) shows the plastic flow of matrix material along the erosion direction for the composite eroded at lower impact angle ($\alpha = 30^\circ$). When impacting at such a low angle, the hard erodent particles penetrate the surface and cause material removal mostly by micro-ploughing. It is possible to investigate the particle flow direction easily from the wear trace on the matrix body, which is indicated by an arrow in this micrograph. The higher impact speed of 58 m/s (Figure 7(b)) makes the sample surface remarkably rough compared to the lower impact speed of 32 m/s (Figure 7(a)). Subsequently the material removal becomes faster. The wear trace is distinctly visible, and the protrusion of fibers beneath the matrix layer is seen. Figure 7(c) shows a portion of the composite surface eroded at an impact angle of 75°. This is the case of maximum material loss due to impact erosion. The SiC particle-filled polyester matrix covering the fiber seems to be chipped off due to repeated impact of hard silica sand particles. A crater thus formed shows an array of almost intact fibers. After the local removal of matrix, this array of fibers is exposed to erosive environment. Figure 7(d) shows fragments of SiC particles and the fibers that are the result of continued sand impact. The broken fiber and carbide filler fragments are mixed with the matrix micro-flake debris, and the damage of the composite is characterized by separation and detachment of this debris.

Steady State Erosion

The erosion wear rates of glass-SiC-polyester composites as a function of the impingement angle (α) are shown in Figure 8. It can be seen that filling of composite with SiC particles reduces the wear rate of the glass-polyester composite quite significantly. The unfilled composite shows maximum erosion occurring at $\alpha_{max} = 60^\circ$ while for both the filled composites (with 10 and 20 wt% SiC content) the value of α_{max} is found to be 75°. It may be mentioned that for ductile materials α_{max} lies usually in the range of 15–30° while for brittle materials the behavior is quite different, i.e., $\alpha_{max} = 90^\circ$ [29]. In the present study, although the thermoplastic polyester is ductile, the location of peak erosion has shifted to 60° from the usual 15–30°, as it is reinforced with glass fiber (curve A). This shift in the erosion behavior is an indication of loss of ductility and is obviously attributed to the brittle fibers. Further shifting of α_{max} from 60 to 75° (curves B and C) proves that the composites tend to become still more brittle with incorporation of SiC particles. The trend is similar for both the composites with SiC filler. It is also important to note that the sample with higher filler content exhibits better

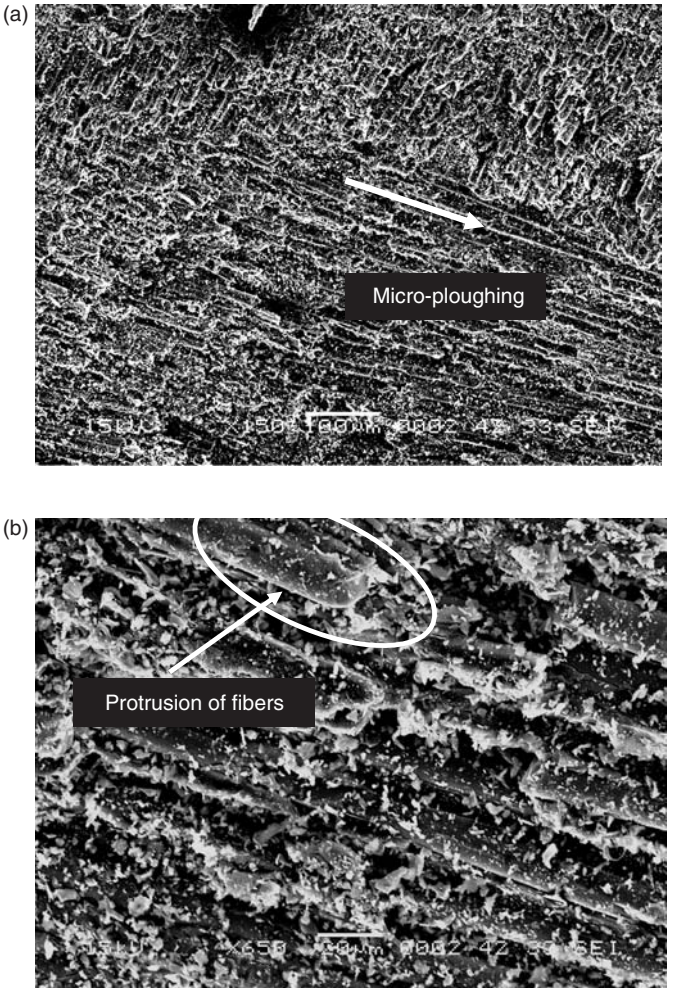

Figure 7. *(a) Scanning electron micrograph of the composite (with 20 wt% SiC) eroded at 30° impingement angle and 32 m/s impact velocity. (b) Scanning electron micrograph of the composite (with 20 wt% SiC) eroded at 30° impingement angle and 58 m/s impact velocity. (c) Scanning electron micrograph of the composite (with 20 wt% SiC) eroded at 75° impingement angle and 58 m/s impact velocity. (d) Magnified scanning electron micrograph of the same composite showing fiber and filler fragmentation.*

erosion resistance. Thus it can be concluded that erosion performance of glass-polyester composites improves with SiC filling, and this improvement is a function of filler content within the limit of the present study.

In Table 2, the last column represents S/N ratio of the erosion rate, which is in fact the average of two replications. The overall mean for the S/N ratio of the erosion rate is found to be -48.45 dB. The analysis was made using the popular software specifically used for design of experimental applications, known as MINITAB 14. Before any attempt is made to use this simple model as a predictor for the measure of performance, the possible interactions between the control factors must be considered. Thus factorial design incorporates a simple means of testing for the presence of the interaction effects.

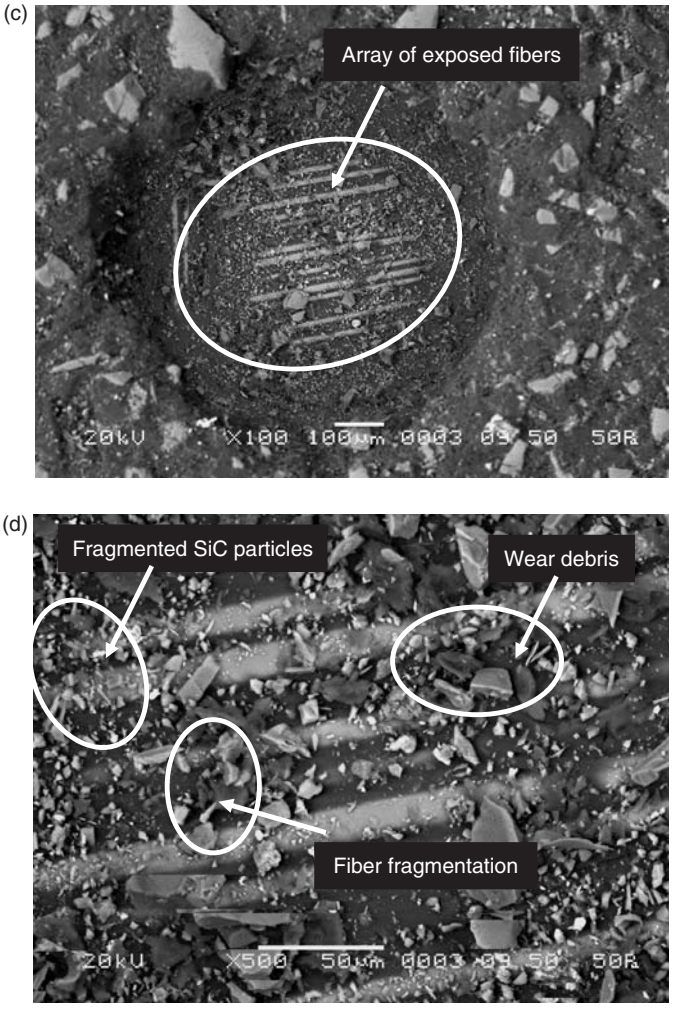

Figure 7. *Continued.*

Analysis of the result leads to the conclusion that factor combination of A_2, B_2, C_3, D_1, and E_2 gives minimum erosion rate. This is evident from Figure 9. As far as minimization of erosion rate is concerned, factors A, B, D, and E have a significant effect whereas factor C has least effect. It is observed from Figure 10 that the interaction between A × B shows the most significant effect on erosion rate. From this analysis we concluded that few of the factors have individual effect on the erosion rate and, similarly, few of the interactions have combined effect on erosion rate.

Similar observation is made in the surface plots of erosion rate with significant control factors (Figure 11(a) and (b)). From this analysis it is concluded that among all the factors, the impingement angle is most insignificant while impact velocity has relatively less significance compared to the other remaining factors. Figure 11(a) shows the significant interaction between impact velocity and SiC percentage for minimization of erosion rate. The main effects plot for S/N ratio for erosion rate indicates the selection of medium SiC percentage (10%), medium impact velocity

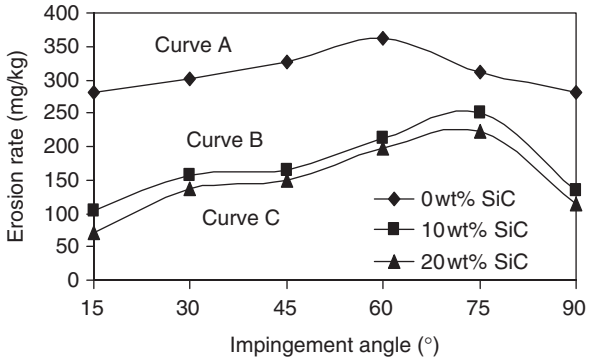

Figure 8. *Erosion rate versus angle of impingement for different SiC filling.*

Table 2. Experimental design using L_{27} orthogonal array.

Expt. No.	Impact velocity (A) (m/s)	SiC percentage (B) (%)	Stand-off distance (C) (mm)	Impingement angle (D)(°)	Erodent size (E) (μm)	Erosion rate (Er) (mg/kg)	S/N ratio (dB)
1	32	0	120	30	300	309.83	−49.8225
2	32	0	180	60	500	235.25	−47.4306
3	32	0	240	90	800	315.19	−49.9714
4	32	10	120	60	500	232.05	−47.3116
5	32	10	180	90	800	269.67	−48.6167
6	32	10	240	30	300	189.80	−45.5659
7	32	20	120	90	800	253.40	−48.0761
8	32	20	180	30	300	299.70	−49.5337
9	32	20	240	60	500	173.28	−44.7750
10	45	0	120	60	800	318.86	−50.0720
11	45	0	180	90	300	349.80	−50.8764
12	45	0	240	30	500	235.25	−47.4306
13	45	10	120	90	300	247.93	−47.8866
14	45	10	180	30	500	132.71	−42.4581
15	45	10	240	60	800	212.63	−46.5525
16	45	20	120	30	500	197.82	−45.9254
17	45	20	180	60	800	288.68	−49.2083
18	45	20	240	90	300	353.83	−50.9759
19	58	0	120	90	500	395.10	−51.9341
20	58	0	180	30	800	215.19	−46.6564
21	58	0	240	60	300	239.89	−47.6002
22	58	10	120	30	800	279.38	−48.9239
23	58	10	180	60	300	293.76	−49.3599
24	58	10	240	90	500	277.38	−48.8615
25	58	20	120	60	300	299.80	−49.5366
26	58	20	180	90	500	495.92	−53.9082
27	58	20	240	30	800	280.63	−48.9627

(45 m/s) and higher stand-off distance (240 mm) results in the best combination to get minimum erosion rate, within the selected range of experiment. Using Figure 9 for S/N ratio, the optimum combination of significant control factors is A_2, B_2, and C_3. Surface response plot Figure 11(c) indicates that the minimum erosion rate can be

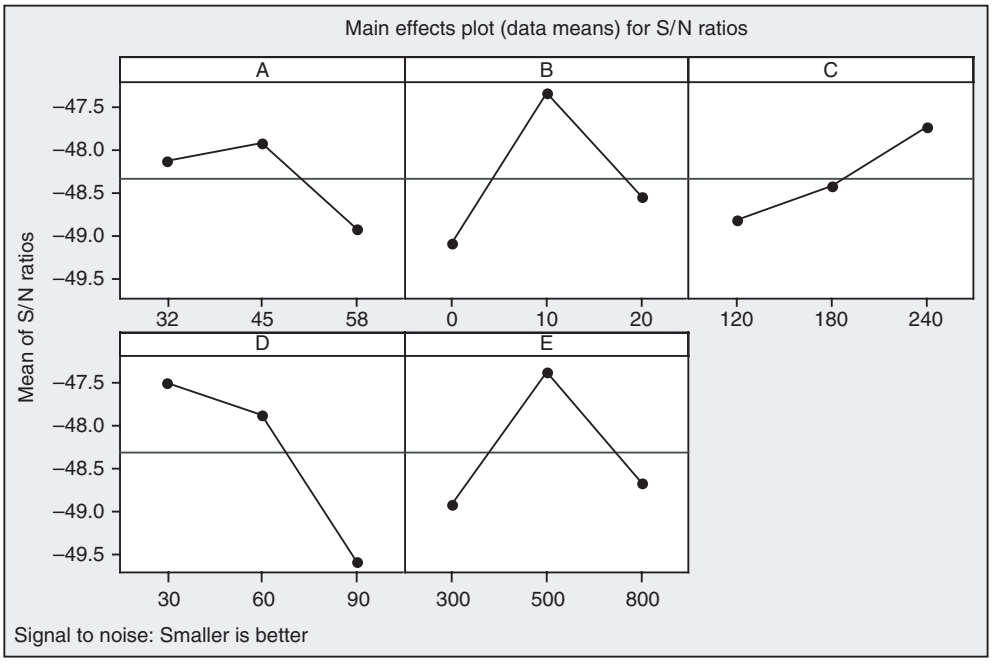

Figure 9. *Effect of control factors on erosion rate.*

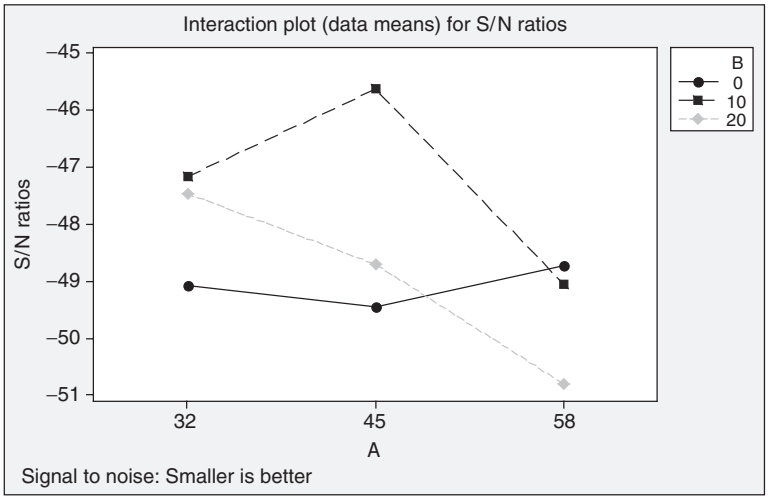

Figure 10. *Interaction graph between A × B for erosion rate.*

achieved in a composite with medium SiC percentage eroded at the medium impact velocity region.

Erosion Efficiency

The hardness alone is unable to provide sufficient correlation with erosion rate, largely because it determines only the volume displaced by each impact and not really the

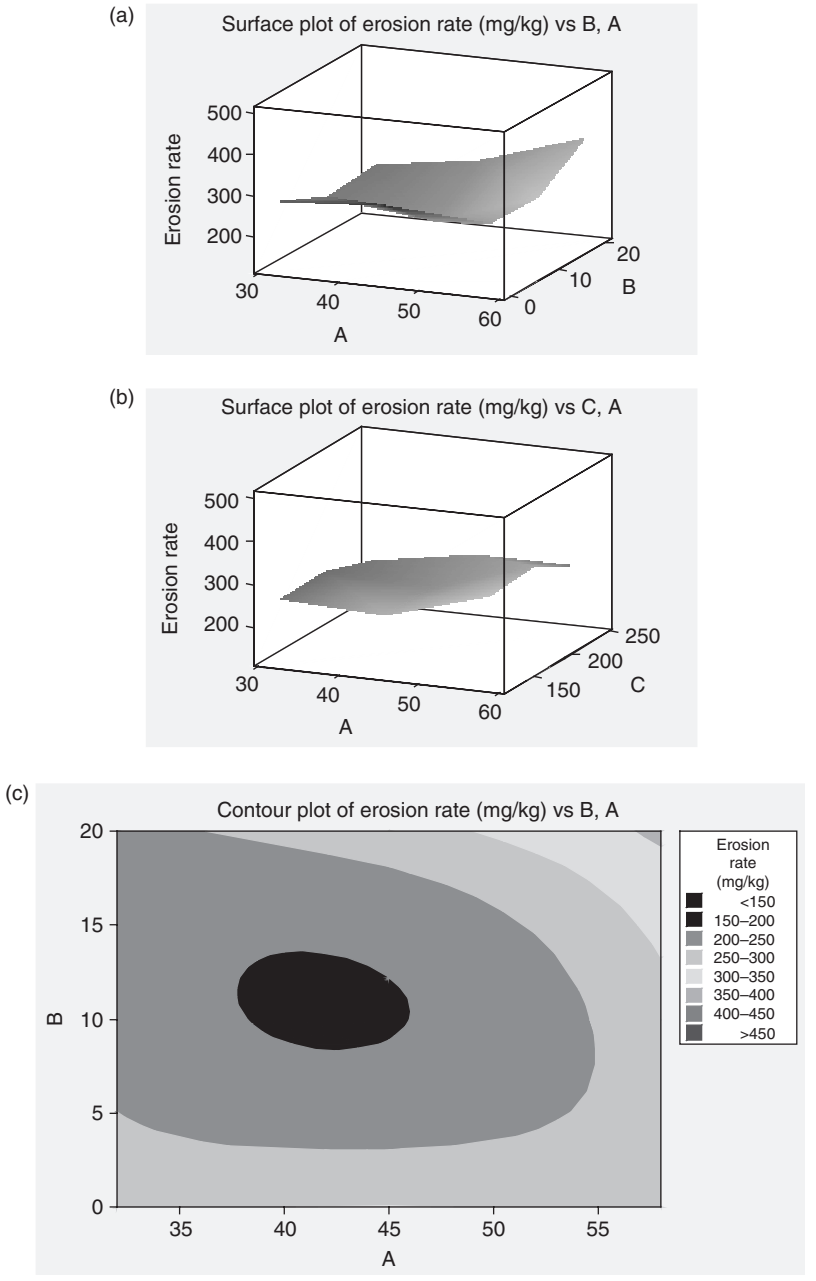

Figure 11. *(a) Surface plot of erosion rate versus A × B interaction. (b) Surface plot of erosion rate versus A × C interaction. (c) Surface response plot.*

volume eroded. Thus a parameter that will reflect the efficiency with which the volume that is displaced is removed should be combined with hardness to obtain a better correlation. The erosion efficiency is obviously one such parameter. In the case of a stream of particles impacting a surface normally (i.e., at $\alpha = 90^{\circ}$), erosion efficiency (η_{normal})

Table 3. Erosion efficiency for different SiC percentages.

Expt. No.	SiC percentage (%)	Impact velocity (V) (m/s)	Density of target material (ρ) (kg/m^3)	Hardness of target material (Hv) (MPa)	Erosion rate (Er) (mg/kg)	Erosion efficiency (η) (%)
1	0	32	1932	39	309.83	47.9189
2	0	32	1932	39	235.25	10.4968
3	0	32	1932	39	315.19	12.1869
4	10	32	1752	43	232.05	12.5889
5	10	32	1752	43	269.67	12.6774
6	10	32	1752	43	189.80	35.6908
7	20	32	1739	47	253.40	13.1181
8	20	32	1739	47	299.70	62.0599
9	20	32	1739	47	173.28	10.3518
10	0	45	1932	39	318.86	7.19456
11	0	45	1932	39	349.80	6.83940
12	0	45	1932	39	235.25	18.3987
13	10	45	1752	43	247.93	5.89392
14	10	45	1752	43	132.71	12.6194
15	10	45	1752	43	212.63	5.83318
16	20	45	1739	47	197.82	20.7142
17	20	45	1739	47	288.68	8.72091
18	20	45	1739	47	353.83	9.26262
19	0	58	1932	39	395.10	4.65023
20	0	58	1932	39	215.19	10.1309
21	0	58	1932	39	239.89	3.25825
22	10	58	1752	43	279.38	15.9918
23	10	58	1752	43	293.76	4.85113
24	10	58	1752	43	277.38	3.96935
25	20	58	1739	47	299.80	5.45187
26	20	58	1739	47	495.92	7.81484
27	20	58	1739	47	280.63	17.6889

defined by Sundararajan et al. [30] is given as:

$$\eta_{\text{normal}} = \frac{2ErHv}{\rho V^2}. \tag{3}$$

But considering impact of erodent at any angle α to the surface, the actual erosion efficiency can be obtained by modifying Equation (3) as:

$$\eta = \frac{2ErHv}{\rho V^2 \sin^2\alpha}. \tag{4}$$

The evaluation of erosion efficiency can be made only on the basis of experimental data. Hence, the values of erosion efficiencies of these composites calculated using Equation (4) are summarized in Table 3, along with their hardness values and operating conditions. It clearly shows that erosion efficiency is not exclusively a material property, but also depends on other operational variables such as impingement angle and impact velocity. The erosion efficiencies of these composites under normal impact (η_{normal}) vary 3–6, 6–9, and 9–12% for impact velocities of 58, 45, and 32 m/s, respectively. The value of η for a particular impact velocity under oblique impact can be obtained simply by multiplying

Table 4. ANOVA table for erosion rate.

Source	DF	Seq SS	Adj SS	Adj MS	*F*	*p*
A	2	15.576	15.576	7.788	2.22	0.171
B	2	18.563	18.563	9.282	2.65	0.131
C	2	4.943	4.943	2.471	0.70	0.523
D	2	40.043	40.043	20.022	5.71	0.029
E	2	7.027	7.027	3.514	1.00	0.409
$A \times B$	4	19.899	19.899	4.975	1.42	0.312
$A \times C$	4	6.819	6.819	1.705	0.49	0.747
Error	8	28.073	28.073	3.509		
Total	26	140.942				

a factor $1/\sin^2\alpha$ with $\eta_{\text{normal.}}$ Similar observation on velocity dependence of erosion efficiency has previously been reported by a few investigators [30,31].

The magnitude of η can be used to characterize the nature and mechanism of erosion. For example, ideal micro-ploughing involving just the displacement of the material from the crater without any fracture (and hence no erosion) will result in $\eta = 0$. In contrast, if the material removal is by ideal micro-cutting, $\eta = 1.0$ or 100%. If erosion occurs by lip or platelet formation and their fracture by repeated impact, as is usually the case in the case of ductile materials, the magnitude of η will be very low, i.e. $\eta \leq 100\%$. In the case of brittle materials, erosion occurs usually by spalling and removal of large chunks of materials, resulting from the interlinking of lateral or radial cracks, and thus η can be expected to be even >100% [26]. The erosion efficiencies of the composites under the present study indicate that at low impact speed the erosion response is semi-ductile ($\eta = 10$–100%). On the other hand, at relatively high impact velocity the composites exhibit ductile ($\eta < 10\%$) erosion behavior [32].

ANOVA and the Effects of Factors

In order to find out statistical significance of various factors like impact velocity (A), SiC percentage (B), stand-off distance (C), impingement angle (D), and erodent size (E), on erosion rate, analysis of variance (ANOVA) is performed on experimental data. Table 4 shows the results of the ANOVA with the erosion rate. This analysis is undertaken for a level of confidence of significance of 5%. The last column of the table indicates that the main effects are highly significant (all have very small *p*-values).

From Table 4, one can observe that erodent size ($p = 0.146$), SiC percentage ($p = 0.131$), impact velocity ($p = 0.171$), and impingement angle ($p = 0.409$) have great influence on the erosion rate. The interaction of impact velocity × SiC percentage ($p = 0.354$) shows significant contribution to the erosion rate but the remaining factors and interactions have relatively less significant contribution to the erosion rate.

CONFIRMATION EXPERIMENT

The optimal combination of control factors has been determined in the previous analysis. However, the final step in any design of experiment approach is to predict and verify improvements in observed values through the use of the optimal combination level of control factors. The confirmation experiment is performed by taking an arbitrary factor

combination $A_1B_3D_2E_3$. Factor C has been omitted because factor C and interaction $A \times C$ have the least effect on erosion rate, as is evident from Table 4. The estimated S/N ratio for erosion rate can be calculated with the help of the following prediction equation:

$$\begin{aligned}\hat{\eta}_1 = \bar{T} + (\bar{A}_1 - \bar{T}) + (\bar{B}_3 - \bar{T}) + [(\bar{A}_1\bar{B}_3 - \bar{T}) - (\bar{A}_1 - \bar{T}) - (\bar{B}_3 - \bar{T})] \\ + (\bar{D}_2 - \bar{T}) + \left(\bar{E}_3 - \bar{T}\right)\end{aligned} \tag{5}$$

where $\bar{\eta}_1$ is the predicted average, $\bar{T}$ is the overall experimental average, and $\bar{A}_1, \bar{B}_3, \bar{D}_2,$ and $\bar{E}_3$ are the mean responses for factors and interactions at designated levels.

By combining like terms, the equation reduces to:

$$\bar{\eta}_1 = \bar{A}_1\bar{B}_3 + \bar{D}_2 + \bar{E}_3 - 2\bar{T}. \tag{6}$$

For a new combination of factor levels, $\bar{\eta}_1 = -47.0984$ dB, through the prediction equation and experimentally it is obtained as -48.4788 dB. The resulting model seems to be capable of predicting erosion rate to a reasonable accuracy since an error of 2.84% is observed. However, the error can be further reduced if the number of measurements is increased. This validates the development of the mathematical model for predicting the measures of performance based on knowledge of the input parameters.

FACTOR SETTINGS FOR MINIMUM EROSION RATE

In this study, an attempt is made to derive optimal settings of the control factors for minimization of erosion rate. The single-objective optimization requires quantitative determination of the relationship between erosion rates with combination of control factors. In order to express the erosion rate in terms of a mathematical model, the following form is suggested:

$$Er = K_0 + K_1 \times A + K_2 \times B + K_3 \times D + K_4 \times E + K_5 \times A \times B. \tag{7}$$

Here, Er is the performance output terms and K_i ($i = 0, 1, \ldots, 5$) are the model constants. The constants are calculated using non-linear regression analysis with the help of SYSTAT 7 software and the following relations are obtained:

$$\begin{aligned}&Y = 0.413 - 0.021 \times A - 0.412 \times B + 0.275 \times D - 0.047 \times E + 0.540 \times A \times B \\ &r^2 = 0.96.\end{aligned} \tag{8}$$

The correctness of the calculated constants is confirmed as high correlation coefficients (r^2) to the tune of 0.96 obtained for Equation (7) and, therefore, the models are quite suitable to use for further analysis.

It is indeed a challenging task to find optimal settings of the control factors for minimization of erosion rate because the search is to be made in a large experimental region under constraints of parameter values. However, genetic algorithms (GAs), which are capable of simulating natural evolution processes and guarantee global optimum, can be successfully used.

Here, the resultant objective function to be maximized is given as:

$$\text{Maximize } Z = \frac{1}{f}. \tag{9}$$

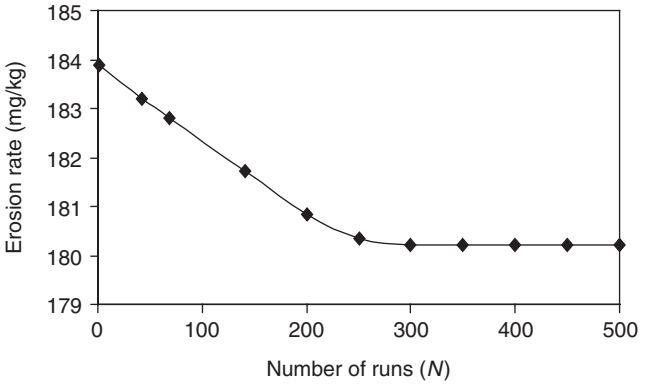

Figure 12. *Convergence curve.*

Normalized function for erosion rate where subjected to constraints:

$$A_{\min} < A < A_{\max} \tag{10}$$

$$B_{\min} < B < B_{\max} \tag{11}$$

$$D_{\min} < D < D_{\max} \tag{12}$$

$$E_{\min} < E < E_{\max}. \tag{13}$$

The min and max in Equations (15)–(18) show the lowest and highest control factor settings (control factors) used in this study (Table 1). In genetic optimization, population size, probability of crossover and mutation are set at 50, 75, and 5%, respectively. The number of generations is increased until the output is converged. In order to obtain a minimum erosion wear rate of 368.96 mg/kg, impact velocity, SiC percentage, impingement angle, and erodent size must be set at 57.07 m/sec, 18.26%, 88.11°, and 444.80 μm. The pattern of convergence of performance output with number of generations is shown in Figure 12.

CONCLUSIONS

Based on the studies made on erosion characteristics, the following conclusions are drawn:

- Successful fabrication of glass fiber and SiC-reinforced polyester matrix composites is possible by simple hand lay-up techniques. Such composites have adequate potential for applications in highly erosive environments. Although they exhibit poorer tensile and flexural strength, their erosion wear performance shows significant improvement with the addition of SiC filler.
- The peak erosion rate shifts to a larger value of impingement angle ($\alpha_{\max} = 75°$) compared to ductile materials, due to the brittle nature of glass fiber and reinforced SiC particles. This indicates the semi-ductile nature of the composites.
- Erosion response of these composites is successfully analyzed using the Taguchi experimental design scheme.

- Factors like erodent size, SiC percentage, impact velocity and impingement angle, in order of priority, are found to be significant to minimize the erosion rate. Although the effect of impact velocity is less compared to other factors, it cannot be ignored because it shows significant interaction with another factor, i.e. the percentage of SiC in the composite.
- The erosion efficiency (η), in general, characterizes the wear mechanism of composites. The SiC-filled GF-polyester composites exhibit semi-ductile erosion response ($\eta = 10$–60%) for low impact velocities and ductile erosion response ($\eta < 10\%$) for relatively high impact velocity.
- The rationale behind the use of genetic algorithm lies in the fact that genetic algorithm has the capability to find the global optimal parameter settings whereas the traditional optimization techniques are normally stuck at the local optimum values. The optimum settings are found to be impact velocity = 57.07 m/s, SiC percentage = 18.26, impingement angle = 88.11, erodent size = 444.8 çm, and resulting erosion rate = 368.96 mg/kg as far as present experimental conditions are concerned.

This study leaves a wide scope for future investigations. It can be extended to newer composites using other ceramic fillers and the resulting experimental findings can be similarly analyzed.

REFERENCES

1. Cirino, M., Pipes, R. B. and Friedrich, K. (1987). The Abrasive Wear Behaviour of Continuous Fibre Polymer Composites, *Journal of Materials Science*, **22**: 2481.
2. Wang, Q. H., Xue, Q. J., Liu, W. M. and Chen, J. -M. (2000). The Friction and Wear Characteristics of Nanometer SiC and PTFE filled PEEK, *Wear*, **243**: 140.
3. Cirino, M., Friedrich, K. and Pipes, R. B. (1988). Evaluation of Polymer Composites for Sliding and Abrasive Wear Application, *Composites*, **19**: 383.
4. Lhymn, C., Tempelmeyer, K. E. and Davis, P. K. (1985). The Abrasive Wear of Short Fibre Composites, *Composites*, **16**: 127.
5. Voss, H. and Friedrich, K. (1987). On the Wear Behaviour of Short Fibre Reinforced PEEK Composites, *Wear*, **116**: 1.
6. Briscoe, B. J., Yao, L. H. and Stolarski, T. A. (1986). The Friction and Wear of PTFE and PEEK Composites: An Initial Appraisal of the Optimum Composition, *Wear*, **108**: 357.
7. Bahadur, S. and Gong, D. (1992). The Role of Copper Compounds as Fillers in the Transfer and Wear Behaviour of PEEK, *Wear*, **154**: 151.
8. Wang, Q. H., Xue, Q. J., Shen, W. C. and Zhang, J. (1998). The Friction and Wear Properties of Nanometer ZrO_2-Filled PEEK, *Journal of Applied Polymer Science*, **69**: 135.
9. Wang, Q. H., Xue, Q. J. and Shen, W. C. (1998).The Tribological Properties of SiC Whisker Reinforced PEEK, *Journal of Applied Polymer Science*, **69**: 2341.
10. Gregory, S. W., Freudenberg, K. D., Bhimaraj, P. and Schadler, L. S. (2003). A Study on the Friction and Wear Behavior of PTFE Filled with Alumina Nanoparticles, *Wear*, **254**: 573–580.
11. Jung-Il, K., Kang, P. H. and Nho, Y. C. (2004). Positive Temperature Coefficient Behavior of Polymer Composites Having a High Melting Temperature, *Journal of Applied Polymer Science*, **92**: 394–401.
12. Nikkeshi, S., Kudo, M. and Masuko, T. (1998). Dynamic Viscoelastic Properties and Thermal Properties of Powder-Epoxy Resin Composites, *Journal of Applied Polymer Science*, **69**: 593–598.
13. Zhu, K. and Schmauder, S. (2003). Prediction of the Failure Properties of Short Fiber Reinforced Composites with Metal and Polymer Matrix, *Computation Material Science*, **28**: 743–758.
14. Rusu, M., Sofian, N. and Rusu, D. (2001). Mechanical and Thermal Properties of Zinc Powder Filled High Density Polyethylene Composites, *Polymer Testing*, **20**: 409–417.
15. Tavman, I. H. (1997). Thermal and Mechanical Properties of Copper Powder Filled Poly (ethylene) Composites, *Powder Technology*, **91**: 63–76.

16. Rothon, R. N. (1999). Mineral Fillers in Thermoplastics: Filler Manufacture and Characterization, *Advances in Polymer Science*, **139**: 67–107.
17. Rothon, R. N. (1997). Mineral Fillers in Thermoplastics: Filler Manufacture, *Journal Adhesion*, **64**: 87–109.
18. Mahapatra, S. S. and Patnaik, A., (2006). Optimization of Wire Electrical Discharge Machining (WEDM) Process Parameters using Genetic Algorithm, *International Journal of Advance Manufacturing Technology*, DOI.10.1007/s00170-006-0672-6.
19. Mahapatra, S. S. and Patnaik, A., (2006). Parametric Analysis and Optimization of Drilling of Metal Matrix Composites Based on the Taguchi Method, *The International Journal for Manufacturing Science and Technology*, **8**: 5–12.
20. Patnaik, A., Biswas, S. R. and Mahapatra, S. S. (2007). An Evolutionary Approach for Parameter Optimization of Submerged Arc Welding in Hard Facing Process, *International Journal of Manufacturing Research*, **2**(4): 462–483.
21. Patnaik, A., Satapathy, A., Mahapatra, S. S. and Dash, R. R. (2007). Modeling and Prediction of Erosion Response of Glass Reinforced Polyester-Flyash Composites, *Journal of Reinforced Plastics & Composites*. (In Press).
22. Patnaik, A., Satapathy, A., Mahapatra, S. S. and Dash, R. R. (2007). A Taguchi Approach for Investigation of Erosion of Glass Fiber–Polyester Composites, *Journal of Reinforced Plastics & Composites*. (In press).
23. Patnaik, A., Satapathy, A., Mahapatra, S. S. and Dash, R. R. (2007). Parametric Optimization of Erosion Wear of Polyester-GF-Alumina Hybrid Composites using Taguchi Method, *Journal of Reinforced Plastics & Composites*. (In press).
24. Aglan, H. A. and Chenock Jr, T. A. (1993). Erosion Damage Features of Polyimide Thermoset Composites, *SAMPEQ*: 41–47.
25. Srivastava, V. K. and Pawar, A. G. (2006). Solid Particle Erosion of Glass Fiber Reinforced Flyash Filled Epoxy Resin Composites, *Composite Science and Technology*, **66**: 3021–3028.
26. Suresh, A., and Harsha, A. P. (2006). Study of Erosion Efficiency of Polymers and Polymer Composites, *Polymer Testing*, **25**: 188–196.
27. Glen, S. P. (1993). *Taguchi Methods: A Hands on Approach*., Addison-Wesley, New York.
28. Zhou, R., Lu, D. H., Jiang, Y. H. and Li, Q. N. (2005). Mechanical Properties and Erosion Wear Resistance of Polyurethane Matrix Composites, *Wear*, **259**: 676–683.
29. Rattan, R. and Bijwe, J. (2007). Influence of Impingement Angle on Solid Particle Erosion of Carbon Fabric Reinforced Polyetherimide Composite, *Wear*, **262**: 568–574.
30. Sundararajan, G., Roy, M. and Venkataraman, B. (1990). Erosion Efficiency – A New Parameter to Characterize the Dominant Erosion Micromechanism, *Wear*, **140**: 369.
31. Mishra, P. K. (1997). *Nonconventional Machining*, Narosa Publishing House, New Delhi.
32. Manish Roy, Vishwanathan, B. and Sundararajan, G. (1994). The Solid Particle Erosion of Polymer Matrix Composites, *Wear*, **171**: 149–161.